Video Article

Detection and Recovery of Palladium, Gold and Cobalt Metals from the Urban Mine Using Novel Sensors/Adsorbents Designated with Nanoscale Wagon-wheel-shaped Pores

Sherif A. El-Safty[1,2], Mohamed A. Shenashen[1], Masaru Sakai[3], Emad Elshehy[1], Kohmei Halada[1]

[1]National Institute for Materials Science, Japan

[2]Graduate School for Advanced Science and Engineering, Waseda University

[3]Center for Research in Isotopes and Environmental Dynamics, Tsukuba University

Correspondence to: Sherif A. El-Safty at sherif.elsafty@nims.go.jp; sherif@aoni.waseda.jp

URL: https://www.jove.com/video/53044
DOI: doi:10.3791/53044

Keywords: Engineering, Issue 106, Nanoscale scaffolds, wagon-wheel-shaped, sensor/adsorbent, detection, recovery, palladium, gold and cobalt metals, urban mine

Date Published: 12/6/2015

Citation: El-Safty, S.A., Shenashen, M.A., Sakai, M., Elshehy, E., Halada, K. Detection and Recovery of Palladium, Gold and Cobalt Metals from the Urban Mine Using Novel Sensors/Adsorbents Designated with Nanoscale Wagon-wheel-shaped Pores. *J. Vis. Exp.* (106), e53044, doi:10.3791/53044 (2015).

Abstract

Developing low-cost, efficient processes for recovering and recycling palladium, gold and cobalt metals from urban mine remains a significant challenge in industrialized countries. Here, the development of optical mesosensors/adsorbents (MSAs) for efficient recognition and selective recovery of Pd(II), Au(III), and Co(II) from urban mine was achieved. A simple, general method for preparing MSAs based on using high-order mesoporous monolithic scaffolds was described. Hierarchical cubic *Ia*3*d* wagon-wheel-shaped MSAs were fabricated by anchoring chelating agents (colorants) into three-dimensional pores and micrometric particle surfaces of the mesoporous monolithic scaffolds. Findings show, for the first time, evidence of controlled optical recognition of Pd(II), Au(III), and Co(II) ions and a highly selective system for recovery of Pd(II) ions (up to ~95%) in ores and industrial wastes. Furthermore, the controlled assessment processes described herein involve evaluation of intrinsic properties (*e.g.,* visual signal change, long-term stability, adsorption efficiency, extraordinary sensitivity, selectivity, and reusability); thus, expensive, sophisticated instruments are not required. Results show evidence that MSAs will attract worldwide attention as a promising technological means of recovering and recycling palladium, gold and cobalt metals.

Video Link

The video component of this article can be found at https://www.jove.com/video/53044/

Introduction

Driving forces for the booming use of platinum group metals (PGM) are their extraordinary and sometimes exclusive properties, which make them essential components in a broad range of applications. PGMs can play a part in building a sustainable society, and these materials are used in a variety of contemporary applications and products: chemical process catalysis, automotive emissions control, information technology, consumer electronics, fine jewelry, preparation of dental materials, photovoltaic fuel cells, and lithium ion batteries (LIB)[1-10]. Over the past century, worldwide economic changes have been powered by the use of PGMs. Because of the importance of PGMs in clean technologies and high-technology equipment, the use of PGMs has increased dramatically in modern society. Because of the sharp increases in the use of PGMs, particularly in the production of electronic equipment, the accumulation of electronic waste (e-waste) has led to environmental challenges and concerns. Moreover, the recent surge in commodity prices has generated a new interest in the mining of e-wastes[1-4].

E-wastes contain both hazardous materials and valuable palladium, gold and cobalt metals. If e-wastes are disposed of in landfills or not treated in an environmentally sound manner, they may pose a high risk of environmental damage. Palladium, gold and cobalt metals in e-wastes are a sustainable and "green" secondary resource of such metals[5-10]. Therefore, efficient processes for recovering palladium, gold and cobalt metals from e-wastes are urgently needed.

Future advancements in many technological fields will require control of primary metal resources. Because of the growing importance of palladium, gold and cobalt metals in industrial applications and solutions to environmental problems[11-13], developing adsorption/extraction techniques for the recognition and recovery of such metals has become a top priority.

The main precious metals used in electronic products are silver, gold, palladium, platinum, and small quantities of rhodium[4-8]. Recovering palladium and gold has become crucial because of their unique combination of properties in a wide range of industrial applications, economic value, and rare occurrence. Market mechanisms have been influential in increasing the rates of collection and recycling of circuit boards of outdated PCs, TVs, mobile phones, and other electronic devices. Mass-produced consumer components, such as computer motherboards, contain approximately 80 g of Pd and 300 g of Au per ton of e-waste; the corresponding amounts for mobile phone handsets are 130 g of Pd and

200 g of Au per ton of e-waste[5-10]. This urban mine holds immense amounts of these metals (by comparison, Au and Pd are present in extremely low concentrations in rocks (~4 ng/g), soils (1 ng/g), seawater (0.05 µg/L), and river water (0.2 µg/L)[14-16]). To ensure a continuing and reliable supply of palladium, gold and cobalt metals for future technological innovations and new electronic equipment, it is important to develop an efficient and low-cost technology for recycling precious metals from e-waste. Such technology could serve as insurance against a future scarce availability of rare earth ores, which are predicted to be in short supply, or even exhausted, within 100 years.

An element such as cobalt has an essential input to nearly all of the electrochemical storage energy cells such as LIBs[17-19]. Because of the fast growth of information technology and a wide-range utilization of LIBs, the release of LIBs as e-wastes explored a new environmental challenge[18-20]. Therefore, handling these wastes with care by recovering these resources might open a new avenue in the environment and industrial applications.

Several powerful and well-established methodologies and analytical techniques have been used to discriminate and quantify Au(III), Pd(II), and Co(II) in natural ore and industrial waste, including flame and carbon furnace atomic absorption spectrophotometry, ultraviolet-visible (UV-vis) spectrophotometry, neutron activation analysis, and inductively coupled plasma mass spectrometry[14-16,21-27]. Despite their versatility and growing popularity, these analytical techniques suffer from many shortcomings. For example, they usually require careful planning and testing, involve many sample preparation steps to minimize interference from the sample matrix, require sophisticated instrumentation and well-trained individuals, and must be performed under rigorous experimental conditions[17,21]. Moreover, all of these analytical techniques incorporate pre-concentration and separation steps, such as solvent extraction, coprecipitation, ion exchange, and adsorption, to pre-concentrate the target metal ions from the matrix components prior to their determination[20-27]. Moreover, hydrometallurgy and pyrometallurgy techniques are commonly used in the recycle chain in industry[19-22]. Therefore, developing efficient, cost-effective and easy-to-use analytical methods to recover palladium, gold and cobalt metals from natural ore and industrial waste are important both for environmental protection and in the industrial sector[11-13].

New technologies can offer new approaches to chemical analysis and recovery of metals from natural ore and industrial waste. Recent progress has been made in reducing the cost and shortening the time to fabricate optical chemical nanosensors/adsorbents; however, optical adsorbents are still used for specific real-world sensing, extraction, and recovery applications for a wide range of metals[28-36]. Recently, research has focused on tailoring specific solid mesoporous monoliths for use as highly sensitive sensors for the simple and simultaneous naked-eye detection and removal of toxic and precious metal ions, such as mercury and gold ions, from aquatic samples[28-32]. Here, a process for selectively detecting and efficiently recovering Au(III) and Pd(II) from the urban mine was reported; additionally, the process can be applied for the recovery of Co(II) ions from LIBs. Recycling metals by this process should not only serve as a secondary source of Au(III), Pd(II), and Co(II) ions but also reduce environmental pollution. The protocol designs of wagon-wheel-shaped MSAs show, for the first time, evidence of controlled optical recognition of Au(III), Pd(II), and Co(II) ions, and a highly selective system for recovery of Pd(II) ions (up to ~95%) in ores and industrial wastes.

Protocol

1. Fabrication of Wagon-wheel-shaped, Cubic *Ia*3*d* Mesoporous Monolithic Scaffolds

NOTE: Control cubic geometry (preferentially gyroidal *Ia*3*d* symmetry) and micrometric particle surfaces of mesoporous monolithic scaffolds by using triblock copolymer Pluronic P123 [P123; poly(ethylene oxide-*block*-propylene oxide-*block*-ethylene oxide) ($EO_{20}PEO_{70}EO_{20}$)] as a template.

1. Under typical conditions, add P123, pentadecane, and tetramethyl orthosilicate (TMOS) at a mass ratio of 1.6:2:1.2 to HCl/H_2O (pH ~1.0) in a 200-ml round-bottom flask; then shake mixture at 45 °C until forming a homogeneous sol-gel.
2. Connect flask to a rotary evaporator, and evaporate mixture at 45 °C and a starting pressure of 1,023 hPa. Under these conditions, exothermic hydrolysis and condensation of TMOS occur rapidly.
3. Continue evaporation of the mixture for 10-20 min to obtain the optical gel-like wagon-wheel-shaped monolith around the wall of the connect flask [37-39].
4. Dry the flask containing the as-made monolith at 45 °C for 24 hr to complete drying process.
5. Treat dried wagon-wheel-shaped monolith at 450 °C for 8 hr under normal atmospheric conditions.
6. Grind calcined solid monolith completely by using mortar and pestle, and store ground material for later use as a carrier platform in fabrication of MSAs.

2. Characterization of Materials

1. High-resolution transmission electron microscopy (HRTEM)
    1. Disperse 1 mg of sample in 5 ml ethanol solution using an ultrasonic cleaner, and then drop two droplets of sample on a copper grid.
    2. Vacuum-dry the grid for 20 min prior to inserting samples in HRTEM column.
    3. Perform HRTEM using a transmission electron microscope connected to a CCD camera. Record HRTEM micrographs at an acceleration voltage of 200 kV to obtain a lattice resolution of 0.1 nm.

2. N_2 adsorption-desorption isotherms
    1. Pre-treat wagon-wheel-shaped samples at 100 °C for 8 hr under vacuum to equilibrate pressure to 10^{-3} Torr.
    2. Measure N_2 adsorption-desorption isotherms at 77 K using a surface area and pore size analyzer as per the manufacturer's instructions
    3. Determine pore size distribution from adsorption isotherms by using nonlocal density functional theory. Calculate specific surface area (S_{BET}) by using multipoint adsorption data from linear segments of the N_2 adsorption isotherms using Brunauer-Emmett-Teller (BET) theory.

3. Small-angle powder X-ray diffraction (XRD)

1. Measure XRD patterns by using an 18-kW diffractometer and monochromated CuKα radiation, as per the manufacturer's instructions.
2. Record diffractions by using both a graphite monochromator and Göbel mirror detectors with 2θ angles between 0.1° and 6.5°, corresponding to *d*-spacings between 88.2 and 1.35 nm.
3. Grind sample and spread the powder on the sample holder. Confirm resolution of diffraction peaks with standard reproducibility in 2θ (±0.005°). Repeat sample measurement three times with rotation at various angles (15°, 30°, and 45°).

3. Fabrication of Pd(II)-MSA-1, Au(III)-MSA-2, and Co(II)-MSA-3

1. Synthesis of Pd(II)-MSA-1 and Co(II)-MSA-3
   NOTE: Use a pressure-assisted method to direct the modification of wagon-wheel-shaped, cubic *Ia*3*d* monoliths by 1,5-diphenylthiocarbazone dicarboxylate (L1) and 2-nitroso-1-naphthol (L3) ligands (0.1 M EtOH solutions) to fabricate Pd(II)-MSA-1 and Co(II)-MSA-3, respectively.
   1. Add ethanolic 1,5-diphenylthiocarbazone dicarboxylate (L1) or 2-nitroso-1-naphthol (L3) solutions to solid wagon-wheel monoliths into round flask and mix under shaking for 1 min.
   2. Connect flask containing heterogeneous EtOH-L1/solid monolith mixture to a rotary evaporator, and evaporate mixture at 45 °C and a starting pressure of 1,023 hPa.
   3. Connect another flask containing heterogeneous EtOH-L3/solid monolith mixture to a rotary evaporator, and evaporate mixture at 50 °C and a starting pressure of 1,023 hPa. Remove EtOH solution from heterogeneous EtOH-ligand/solid monolith mixture under vacuum at ambient temperature.
   4. Clarify the formation mechanism of ligand-solid (MSA-1 and MSA-3) of physisorbed short-range interactions (*i.e.*, van der Waals and H-bonding interactions) between the abundant hydroxyl groups of the active surface sites of the wagon-wheel-shaped scaffolds and the heteroatom ligands [40,41].
   5. Calculate the amounts of immobilized L1 and L3 as follows: $q_e = (C_0 - C_e)V/m$, where q_e is adsorbed amount, V is solution volume (L), m is mass of the carriers (g), and C_0 and C_e are initial and supernatant probe concentrations, respectively. The amount of immobilized L1 and L3 can be expected to be around 0.09 mmol/g.

2. Synthesis of Au(III)-MSA-2
   NOTE: Apply building blocks protocol to synthesize Au(III)-MSA-2:
   1. Immobilize a 40 ml of 0.1 M ethanol solution of dilauryldimethylammonium bromide (DDAB) into 0.5 g of wagon-wheel-shaped HOM scaffolds using a rotary evaporator to produce wagon-wheel-shaped HOM-DDAB monoliths.
   2. Dissolve 20 mg of hydrophilic6-hydroxy-5-(4-sulfonatophenylazo)-2-naphthalenesulfonic acid disodium salt (L2) ligand in 80 ml of D.I. water. Add 0.5 g of solid HOM-DDAB monoliths. Then remove the H_2O solution through filtration.
   3. Wash HOM-DDAB-L2 with deionized water until no L2 is eluted; then dry sample at 65-70 °C for 4 hr. Note: 0.07 mmol of L2 ligand per gram of HOM scaffold was incorporated into HOM-DDAB[42].
   4. Clarify the formation mechanism of (MSA-2) based on the L2-DDAB-solid interaction.

4. Batch Studies for Detecting Pd(II), Au(III), and Co(II) Ions

1. Immerse 20 mg of wagon-wheel-shaped MSA-1, MSA-2, and MSA-3 in a mixture of Pd(II), Au(III), and Co(II) ions (ion concentration: 2 mg/L); adjust volume to 20 ml and pH to appropriate pH value of 2, 7, and 5.2, respectively.
2. Mechanically shake mixtures in a temperature-controlled water bath at 25 °C for 45 min at a constant agitation speed of 300 rpm.
3. Filter MSAs through 25-mm filter paper; after equilibration, use visual color assessment and reflectance spectra measurements to determine ion concentrations.
4. Determine Pd(II), Au(III), and Co(II) target ion concentrations by comparing reflectance intensities of MSA-1, MSA-2, and MSA-3 at λ_{max} 384, 486, and 537 nm, respectively, during the addition of unknown concentration of target samples with those of standard concentration of target samples.
5. Conduct other experiments using target Pd(II), Au(III), and Co(II) ion concentrations at the optimum pH value of 2, 7, and 5.2, respectively, using UV-vis spectroscopy. The part per million (ppm, mg/L), part per billion (ppb, µg/L), and molar (mol/L) units are used to define the target ion concentration in solution.

5. Method for Removing Pd(II), Au(III), and Co(II) Ions

1. Immerse 40 mg of each wagon-wheel-shaped MSA in a mixture of specific Pd(II), Au(III), and Co(II) ion concentrations; adjust pH of mixture to specific values of 2, 7, and 5.2, respectively, in a volume of 20 ml, and stir mixture for 2 hr at RT.
2. Filter solid MSAs and analyze filtrate by inductively coupled plasma mass spectroscopy (ICP-MS)[28-30].
3. Calculate the Langmuir isotherm based on the following equation[43]:
   $$C_e/q_e = 1/(K_L q_m) + (1/q_m)C_e$$
   where C_e is target ion concentration, q_e is amount of target ion in equilibrated solution, q_m (mg·g^{-1}) is the amount of Pd(II), Au(III), or Co(II) ions removed to form the monolayer coverage, and K_L is the Langmuir adsorption equilibrium constant. For instance, the q_m data indicate the practical removal of the metal ions from the aqueous medium with high adsorption efficiencies (97%-98%). Moreover, K_L values are consistent with the adsorption/desorption rates, indicating fully reversible metal adsorption assays.

6. Formation of Metal-to-ligand Binding Constants in Wagon-wheel-shaped MSAs

1. Determine stability constants (log K_s) of [Pd-$(L1)_2$], [Au-(L2)], and [Co-$(L3)_2$] complexes at pH 2, 7, and 5.2, which can be expected to be around 5.8, 4.9, and 7.9, respectively.
2. Calculate stability constants according to the following equation[28-32]:
   log K_s = ($[ML]_S/[L]_S$) × [M]
   where [M] is the concentration of free Pd(II), Au(III), or Co(II) ions in solution; [L] represents the concentration of free L (*i.e.*, L not bound to the Pd(II), Au(III), or Co(II) ions); and subscript S refers to the total concentration of the Pd(II), Au(III), or Co(II) ions in the solid phase of the wagon-wheel-shaped MSA.
3. Determine limits of detection (LOD) of MSAs for Pd(II), Au(III), and Co(II) ions as follows:
   LOD = 3σ/Ψ
   where σ and Ψ are the standard deviation and the slope of the calibration graph[40-42].

7. Selective-ion-extraction Experimental System

NOTE: Ensure specific and strong metal-to-ligand binding as follows:

1. Adjust pH of extracted solution to 2, 7, and 5.2 for the Pd(II), Au(III), and Co(II) ions. Alter concentrations of interfering metal ions to ≤5 times greater than the concentrations of the Pd(II), Au(III), and Co(II) target ions. Add a 2 ml of complex-forming agent (*e.g.*, 0.3-0.5 M citrate/tartrate) to the extracted solution prior to the addition of target ions to restrain actively reacting Cu(II) ions.

8. Real Extraction of Metals from Urban Mine

1. Dissolve the PCI board in strong acids to get the metal ions in solution.
2. Add MSAs to the solution containing Pd(II), Au(III), and Co(II) ions to extract these ions into solid MSAs.
3. Filter solid MSAs and analyze filtrate by ICP-MS.

Representative Results

Periodic gyroidal cubic *Ia*3*d* monolithic scaffolds and wagon-wheel-shaped MSAs with large cylindrical open pores (up to 10 nm in diameter) were fabricated using pressure-assisted direct templating with a P123 copolymer microemulsion system. TEM micrographs of the MSAs show wagon-wheel-like channels organized in large domain sizes and in different orientational geometries in the gyroidal bicontinuous cubic *Ia*3*d* mesostructures (**Figure 1**). Although the L1, L2, and L3 probes were directly physisorbed into the monolithic scaffolds (~80 mg of probe per gram of scaffold), the MSAs provided control over potential leaching out of the ligands upon washing, sensing condition assays, and chemical treatment during regeneration/reuse cycles.

Wagon wheel shape-like pores featured the cubic *Ia*3*d* structures of the MSAs, as evidenced by the TEM images (**Figure 1**). The HRTEM micrographs recorded along the dominant facet in the [111] direction indicate the formation of cubic bi-continuous surface morphology[37-39]. Six-fold symmetric channels with different nano-sized interconnections in wagon wheel shape-like pores were characteristics the cubic *Ia3d* lattice structures of MSAs (**Figure 1**, center)[44]. Furthermore, the agreement in the unit cell lattice determining by TEM micrographs (22.5 nm) with the unit cell parameter determined by small-angle XRD ($a = d_{211}\sqrt{6}$) indicates the formation of the cubic Ia3d MSA morphology.

The appearance of pores of various geometrical shapes in this six-fold orientation around each wagon wheel pattern is the key feature of controlled Pd(II), Au(III), and Co(II) ion diffusion, adsorption, and recovery. **Figure 2B** indicates that uniformly shaped pore geometries and textural properties of the cubic *Ia*3*d* MSA-1, MSA-2, and MSA-3 were retained (surface area (S_{BET}) of 560, 520, and 570 m^2/g; pore volume (V_p) of 1.03, 0.98, and 1.09 cm^3/g; and pore size (*D/nm*) of 8.2, 8.1, and 8.2 nm, respectively, as evidenced from N_2 isotherm results). This retention of cubic *Ia*3*d* MSA structural integrity was used for the rational design of the MSAs, for which the Pd(II), Au(III), and Co(II) ions were detected with a fast response time, even at nanomolar concentrations (**Figure 3-5**). A sizeable number of organic moieties with potential functional active sites are strongly anchored onto the wagon wheel pore surfaces via H-bonding and dispersive interactions with retention of the cubic *Ia*3*d* geometry, as evidenced by the Bragg reflection planes (*hkl*) (**Figure 2A**). The formation of stable organic-inorganic hybrid MSAs with suitable accommodation of L1, L2, and L3 into the wagon wheel pores might lead to no leaching of ligands during the metal ion sensing/capture/removal assays and reusability/recovery process.

The specificity and sensitivity of the wagon-wheel-shaped MSAs for the target Pd(II), Au(III), and Co(II) ions were controlled by adjusting the pH to 2, 7, and 5.2, respectively. These specific pH values are the most suitable for the selective, sensitive, and efficient monitoring and removal of metal ions using MSAs (**Figure 6A**). The quantification procedure for sensing/capturing Pd(II), Au(III), and Co(II) ions with MSA-1, MSA-2, and MSA-3 involved detecting changes in color intensity at color response times (R_t) of 2, 3, and 5 min, respectively. To evaluate the sensitivities of the MSAs, color transitions in the reflectance spectra that could be detected by the human eye were carefully monitored over a wide range of metal ion concentrations (0-5,000 µg/L). **Figures 6B-D** show changes in color and reflectance intensity of MSA-1, MSA-2, and MSA-3 at λ_{max} 384, 486, and 537 nm, respectively. These changes indicate metal-to-ligand binding events during the formation of the octahedral [Pd-$(L1)_2$], square-planar [Au-(L2)], and octahedral [Co-$(L3)_2$] complexes (the stability constants of these complexes are higher than those of competing-ion complexes; **Figure 7**).The reflectance spectral responses of the MSAs indicated the efficient detection/recognition of metals. In addition, **Figure 6F** shows that MSAs are very effective in removing and monitoring Pd(II), Au(III), and Co(II) ions from the urban mine and LIB solutions over a wide range of concentrations (from µg/L to mg/L) and even at the low-concentration limits of 0.19, 0.6, and 0.51 µg/L, respectively.

The ion-sensing/ion-removal efficiencies of the wagon-wheel-shaped MSAs toward Pd(II), Au(III), and Co(II) ions in the absence and in the presence of interfering ions were evaluated (**Figure 7**). Significant changes in the visible color patterns and reflectance spectra were evident, in most cases, upon addition of 1 to 18 competing ions [*i.e.,* (G1) of K(I), Na(I), Li(I), Ca(II), Fe(III), and Cu(II); (G2) of Cd(II), Pb(II), Hg(II),

Ni(II), Mn(II), Al(III); and (G3) of Bi(III), Zn(II), Dy(III), Er(III), Ho(III), and La(III)]to the Pd(II), Au(III), and Co(II) ion systems, confirming selective removal and efficient monitoring of the target (T) ions. Low concentrations of Ni(II), Cu(II), and Fe(III) ions interfered, but interferences were eliminated by using 0.3-0.5 M citrate/tartrate solution as a suppressing agent; no significant changes in the visible color patterns and reflectance spectra occurred upon addition of high concentrations of various cations at the optimal ion-sensing/capture conditions (pH 2, 7, and 5.2, 40 mg of the MSAs, 20 ml volume, 25 °C) (**Figure 7**). These findings indicated selective identification and capture of target ions in a wide range of real samples containing high concentrations of competing ions[45,46].

The reusability of the wagon-wheel-shaped MSAs was assessed by examining the reflectance spectra of the target ion sensing/capture assays and determining the uptake efficiency (*E* %) as a function of regeneration/reuse cycle. The recycling process was carried out by stripping the Pd(II), Au(III), and Co(II) ions from the MSA surfaces (*i.e.*, decomplexation). Decomplexation was accomplished by treating the Pd(II)-, Au(III)-, and Co(II)-MSAs with 0.1 M $HClO_4$, 0.1 M thiourea in 1% concentrated HCl, and 2M HCl, respectively. The decomplexation treatment was carried out repeatedly to completely remove the Pd(II), Au(III), and Co(II) ions from the MSA surfaces. UV-vis spectroscopy and ICP-MS were used to confirm that the MSA surfaces were free of metal (**Figure 8**). Uptake efficiencies for MSA-1, MSA-2, and MSA-3 were calculated as % (C_A/C_0), where C_A is the target ion concentration uptake by solid MSAs and C_0 is the initial target ion concentration. Results indicated that the functionalities of the wagon-wheel-shaped MSAs were maintained over eight regeneration/reuse cycles[46,47].

The recovery of Pd(II) and Au(III) from electronic scrap (*i.e.,* PCI boards) and Co(II) from LIBs was carried out in several stages:

The first stage was the mechanical separation of grinded PCI board components.

The second stage included a pretreatment hydrometallurgical process, in which the PCI board chips (e-waste source) were leached in a mixture of 2 M H_2SO_4 and 0.2 M H_2O_2 at 90 °C for 6 hr to dissolve base metals (Cu, Fe, Ni, Al, Li, Mn, Co and Zn) and a suspension of partially dissolved plastic and Pd(II) and Au(III) ions[8]. After filtration of undissolved plastics, the residue was leached with a combined acid of HCl and HNO_3 (3:1)at 70 °C for 3 hr to form a soluble solution of Pd(II), Au(III), Ag(I), Fe (III), Sn(IV) and Al(III) ions. The Fe (III), Sn(IV) and Al(III) ions precipitate by raising pH solution up to 4.5 using 2 M NaOH and filtered off. AgCl was precipitated using NaCl and filtered off (**Figure 9**). Additionally, the LIBs waste components were treated with HNO_3, leading to a mixture of Co(II), Ni(II), Mn(II), Li(I), Fe(III), and Al(III) ions.

The third stage involved a series of batch experiments carried out under controlled experimental conditions. In these experiments, leach solutions were purified, Pd(II) and Au(III) ions were recovered from the electronic scrap solutions using MSA-1 and MSA-2 (see **Figure 9**), and Co(II) was recovered from the main products of the LIB solution using MSA-3 (**Table 1**). After removal, the filtrate was analyzed by ICP-MS.

In the fourth stage, the percentage uptakes of Pd(II) and Au(III) by MSA-1 and MSA-2 from a real urban mine composite mixture [0.119 mg/L Pd(II), 0.35 mg/L Au(III), 0.23 mg/L Ag(I), 7.05 mg/L Cu(II), 5.78 mg/L Ni(II), 13.35 mg/L Fe(III), 7.09 mg/L Al(III)] were determined. MSA-3 was used to estimate the recovery of Co(II) ions from a real LIB composite mixture [1.75 mg/L Co(II), 420 mg/L Ni(II), 350 mg/L Mn(II), 370 mg/L Li(I), 7 mg/L Fe(III), 1 mg/L Al(III)]. The efficiency of uptake of Pd(II), Au(III), and Co(II) ions by MSA-1, MSA-2, and MSA-3 was calculated as follows: $E\% = C_A/C_e = C_0 - C_e/C_0$, where C_A is the target ion concentration uptake by solid MSAs, and C_e and C_0 are the target ion concentrations in the equilibrated and initial solutions. **Table 1** presents results for the real-sample study of the extraction of Pd(II), Au(III), and Co(II) using the MSAs; the percentage uptakes of Pd(II), Au(III), and Co(II) were approximately 79%, 68%, and 66%, respectively.

The fifth stage involved recovery experiments using stripping agents (**Figure 3-5**) to release Pd(II), Au(III), and Co(II) ions from the wagon-wheel-shaped MSA surfaces. The recovery efficiency (*R*%) was calculated as follows: $R\% = C_R/C_A$, where C_R is the target ion concentration released in solution by the stripping agent. ICP-MS analyses of the collected solutions indicated that >>98% of the metal ions were released by simple chemical stripping (**Table 1**). This result indicates that ultra-trace levels of Pd(II), Au(III), and Co(II) ions were extracted from the urban mine by the MSAs .

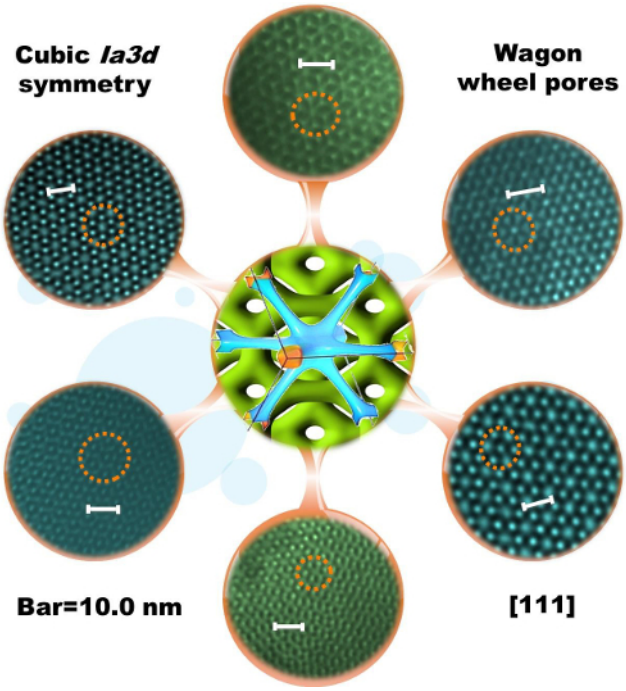

Figure 1. Investigation of wagon-wheel-shaped geometry. HRTEM micrographs of the wagon wheel pattern in the cubic *Ia3d* structures of the MSAs. Center: crystal shape.

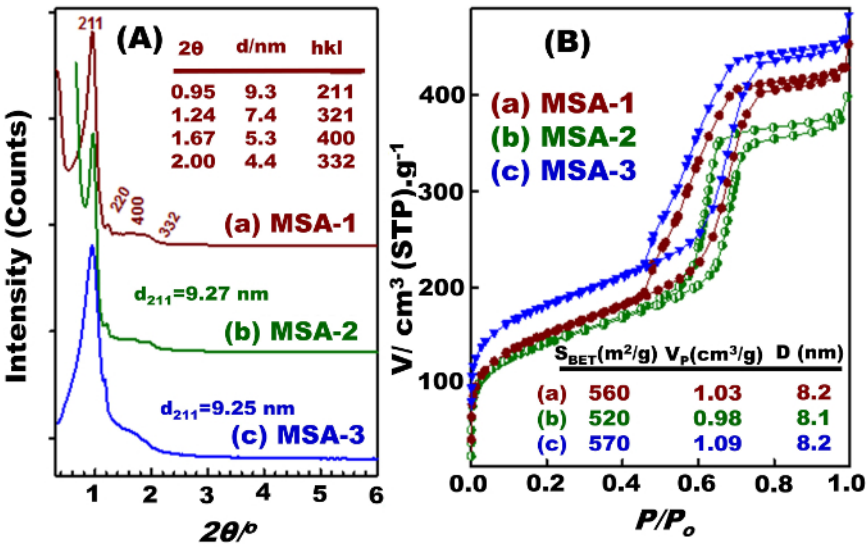

Figure 2. Determination of mesostructured crystal lattice and surface parameters of wagon-wheel-shaped pores. XRD patterns (**A**) and N_2 adsorption/desorption isotherms (**B**) of the wagon-wheel-shaped, cubic *Ia3d* MSAs.

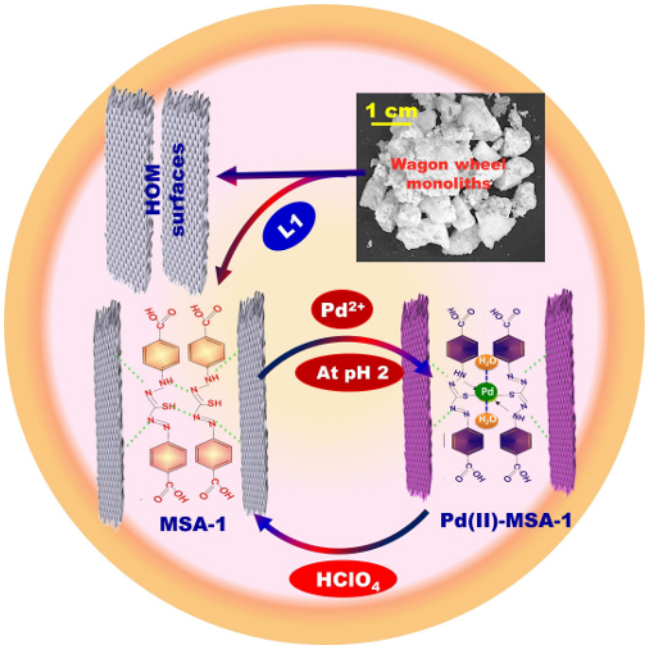

Figure 3. Systematic engineering of the MSA-1. Fabrication of Pd(II)-MSA-1 and Co(II)-MSA-3 via the pressure-assisted method.

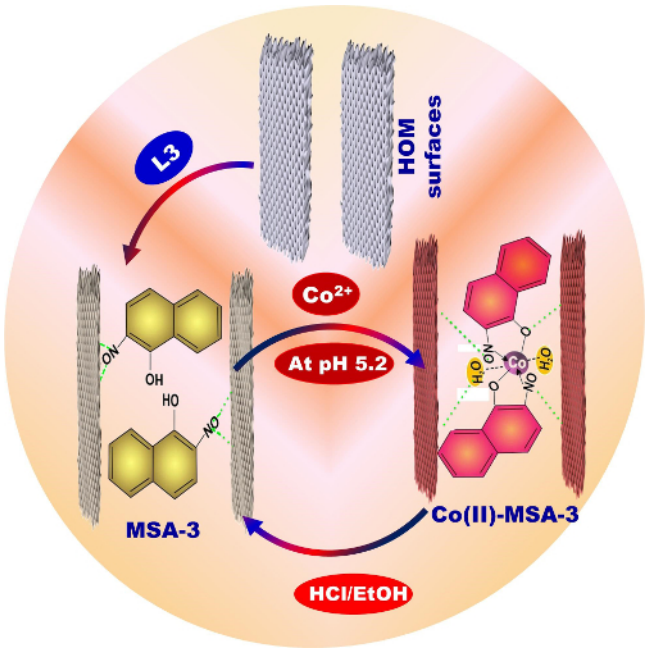

Figure 4. Systematic engineering of the MSA-3. Fabrication of Co(II)-MSA-3 via the pressure-assisted method.

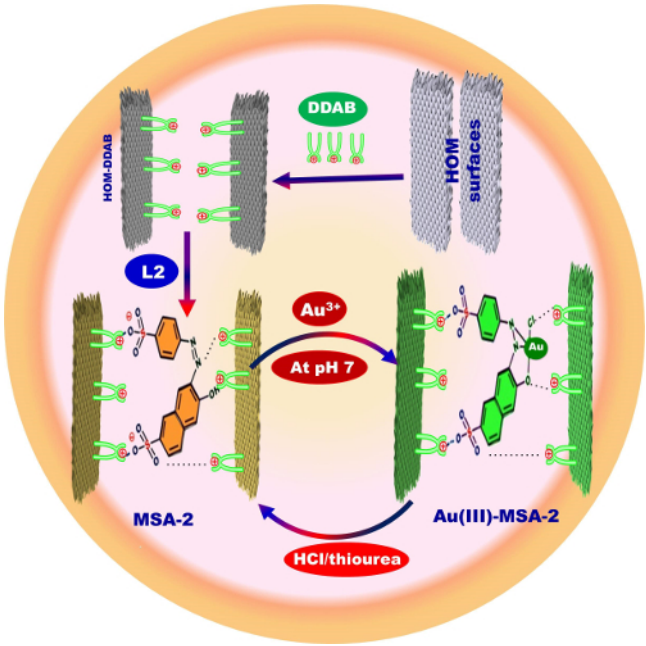

Figure 5. Systematic engineering of the MSA-2. Fabrication of Au(III)-MSA-2 via the building blocks protocol.

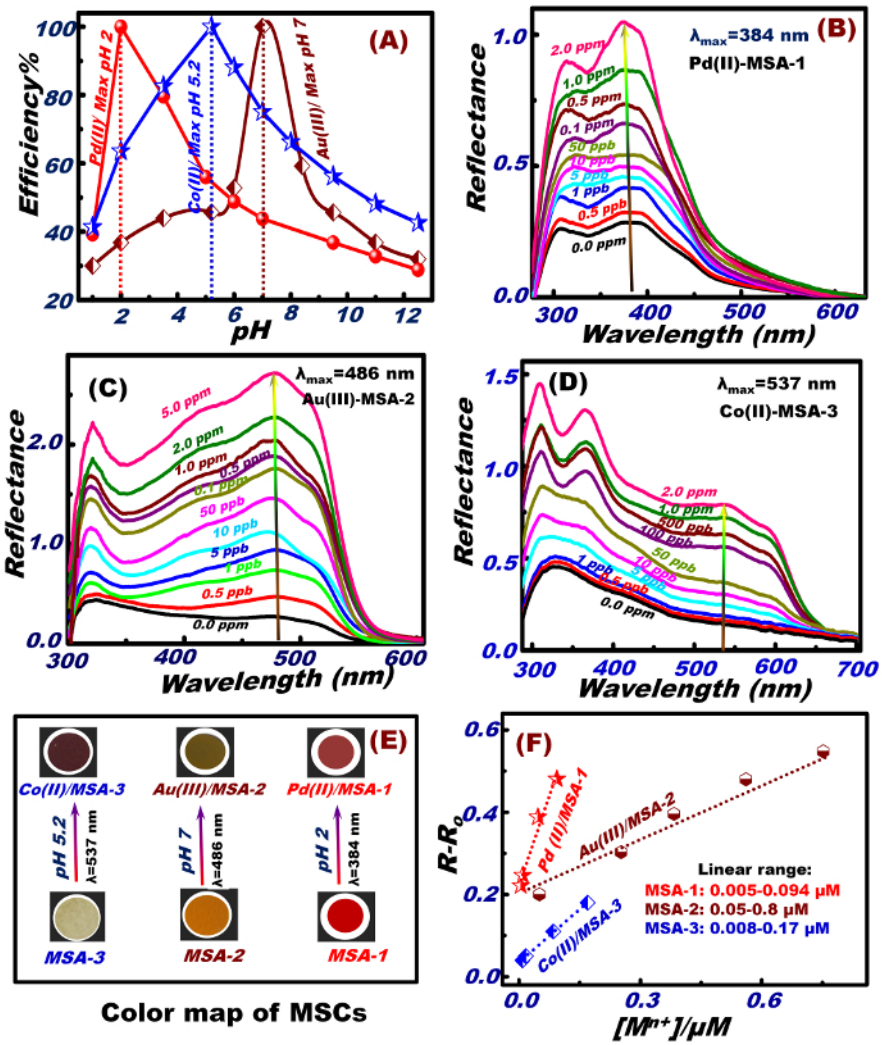

Figure 6. Controlled pH-dependent Pd(II), Au(III), and Co(II) ion-sensing systems. (**A**) pH-response profiles of wagon-wheel-shaped MSA-1, MSA-2, and MSA-3 during the sensing and removal assays of target Pd(II), Au(III), and Co(II) ions. The efficiency of the reflectance spectra was monitored as a function of pH at λ_{max} = 384, 486, and 537 nm, respectively. (**B**-**D**) Target ion concentration as a function of the reflectance spectra of MSA-1, MSA-2, and MSA-3, respectively. (**E**) Color maps for the MSAs with addition of 2 ppm Pd(II), Au(III), and Co(II). (F) Calibration plots of ($R - R_0$) *vs.* [M^{n+}] for MSA-1, MSA-2, and MSA-3. Note: R and R_0 represent the reflectance of the MSAs with and without the addition of target ions, respectively.

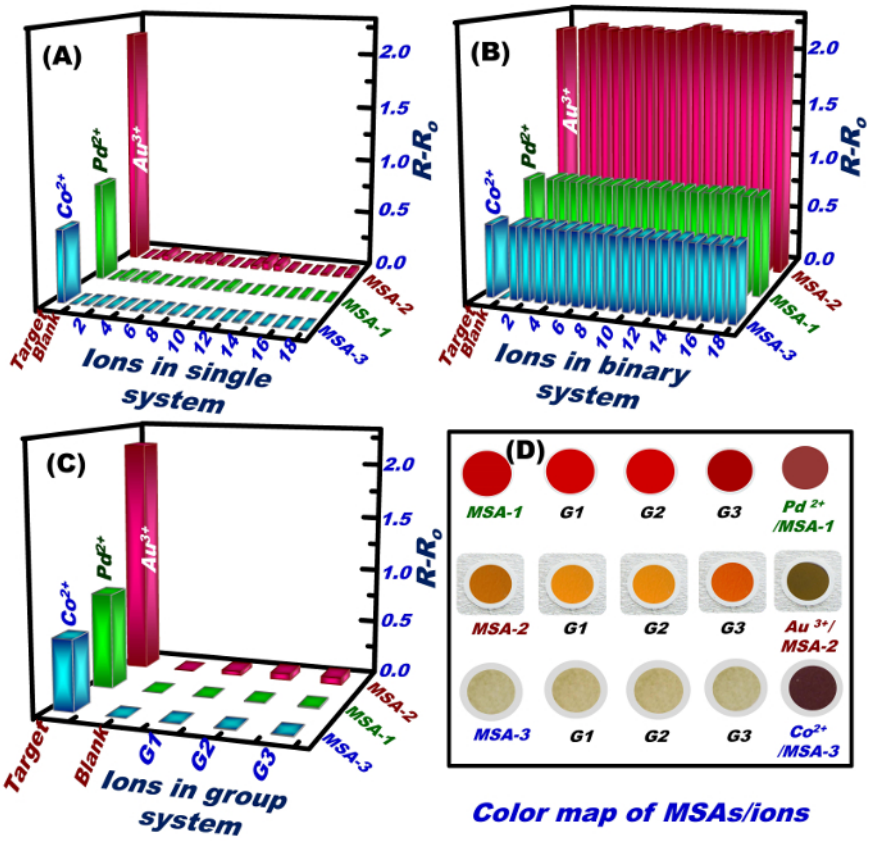

Figure 7. Study of the Pd(II), Au(III), and Co(II) ion-selective systems. (**A**-**C**) Selectivity of wagon-wheel-shaped MSA-1, MSA-2, and MSA-3 toward Pd(II) (2 mg/L), Au(III) (1 mg/L), and Co(II) (2 mg/L) ion-sensing and ion-removal assays. (**D**) Sequential color response ofMSA-1, MSA-2, and MSA-3 (blank; *i.e.,* metal-free assay) toward target Pd(II), Au(III), and Co(II) ions upon addition of interfering ions in single, binary, and groups of ions (G1-G3).

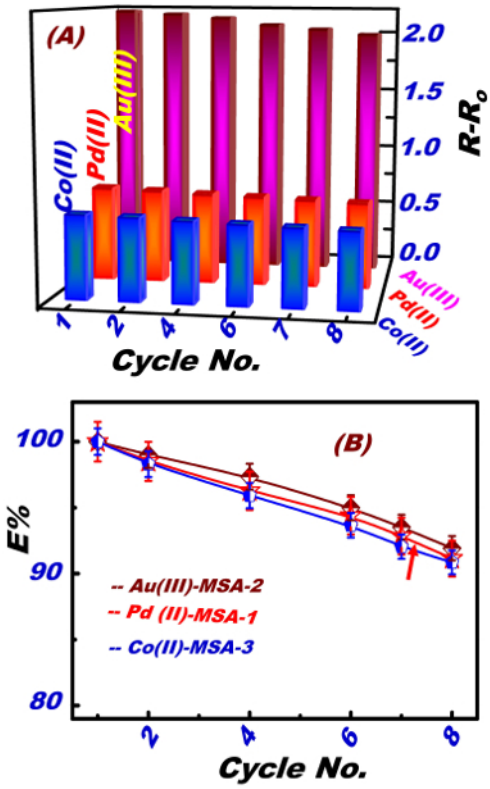

Figure 8. Reusability of wagon-wheel-shaped MSAs. (**A**) Evaluation of the wagon-wheel-shaped, optical sensing/removal assays of the target ions after eight regeneration/reuse cycles (target ion concentration: 2 mg/L; pH and signal response time values for MSA-1, MSA-2, and MSA-3:pH = 2, 7, and 5.2,R_t = 2, 3,and 5 min; t = 25 °C). (**B**) Uptake efficiency *vs.* regeneration cycle number.

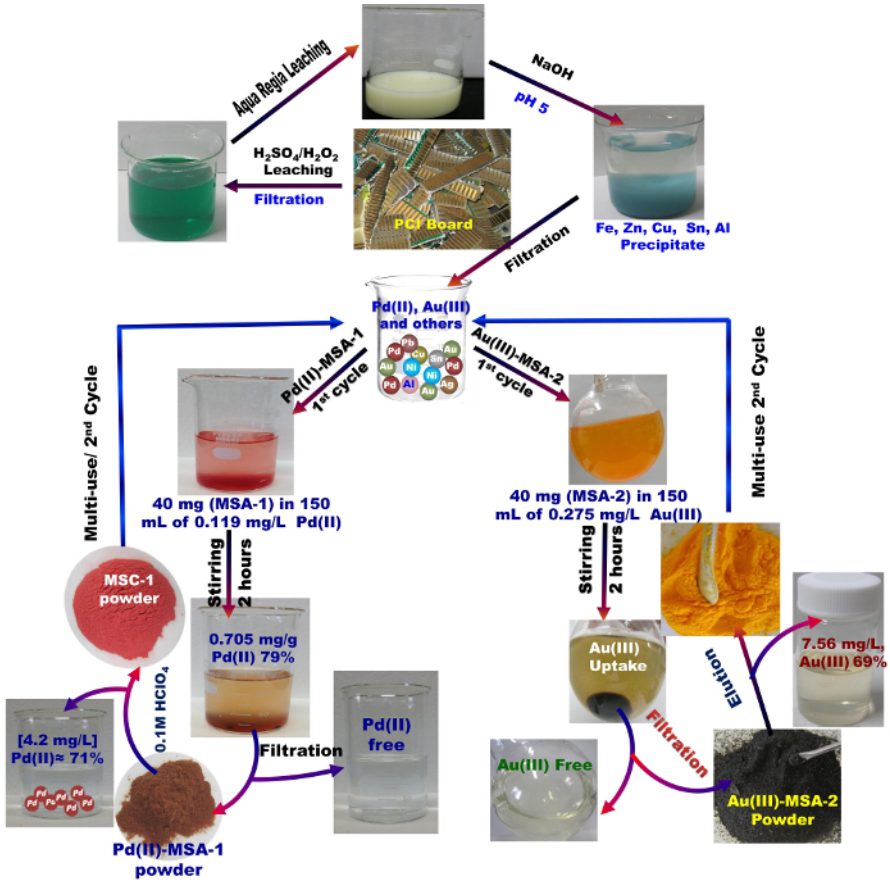

Figure 9. Real recovery of Pd(II) and Au(III) ions from electronic scrap solutions. Hydrometallurgical treatment of PCI boards and recovery of Pd(II) and Au(III) ions from electronic scrap solutions.

Target ions	Target ion-determination	Target ions (mg/L)	Coexisted metal ions (mg/L)	E %	R %
Pd(II)	C_0	0.119	Ag (I): 0.23, Au(III): 0.35, Al(III): 7.09, Ni(II): 5.78, Fe(III): 13.35, Cu(II): 7.05	79	97
	C_e	0.025	Ag (I): 0.225, Au(III): 0.351, Al(III):7.11, Ni(II): 5.77, Fe(III):13.32, Cu(II): 6.95		
	C_R	0.0913	Ag (I): 0.00, Au(III): 0.001, Al(III): 0.00, Ni(II): 0.002, Fe(III): 0.005, Cu(II): 0.009		
Au(III)	C_0	0.35	Ag (I): 0.23, Pd(II): 0.119, Al(III): 7.09, Ni(II): 5.78, Fe(III): 13.35, Cu(II): 7.05	68	98
	C_e	0.11	Ag (I): 0.231, Pd(II): 0.118, Al(III): 7.00, Ni(II): 5.66, Fe(III): 13.29, Cu(II): 6.92		
	C_R	0.235	Ag (I): 0.00, Pd(III): 0.002, Al(III): 0.00, Ni(II): 0.004, Fe(III): 0.003, Cu(II): 0.01		
Co(II)	C_0	1.75	Ni(II): 420, Mn(II): 350, Li(I): 370, Fe(III): 2.00, Al(III): 0.40	66.3	95
	C_e	0.59	Ni(II): 419.34, Mn(II): 350.06, Li(I): 370, Fe(III): 1.91, Al(III): 0.05		
	C_R	1.15	Ni(II): 0.85, Mn(II): 0.00, Li(I): 0.00, Fe(III): 0.05, Al(III): 0.02		

Table 1. Quantitative determination of metal ions in real samples. ICP-MS analytical data for the recovery of Pd(II), Au(III), and Co(II) ions in electronic scrap and LIB solutions.

Discussion

Worldwide demand is growing for a means to accurately and rapidly detect, selectively recognize, and recover Pd(II), Au(III), and Co(II) ions from electronic scrap and LIB solutions. To address this issue, wagon-wheel-shaped, optical MSAs for chemical detection/removal/extraction and recovery of these metal ions were developed.

In designing the MSAs, two key factors were considered as follows: (1) receptors and (2) immobilization/transducing scaffolds. Receptors are organic ligands responsible for the selectivity of the MSAs; scaffolds are responsible for the stability, reusability, and sensitivity of the MSAs. Because of their highly uniform channels, large surface areas, pore size distribution, and controllable wagon-wheel structure, which is commonly associated with the [111] projection of the cubic bicontinuous surface morphology (**Figures 1** and **2**), the MSA-based wagon wheel *Ia3d* mesostructure material scaffolds provided control over the potential demands of this detection/removal/extraction and recovery method

as follows: (1) stability of ligand-embedding HOM solid (*i.e.,* no leaching out of the ligands upon washing), (2) sensing condition assays, and (3) chemical treatment conditions during the regeneration/reuse cycles (*i.e.,* after eight cycles); high ligand-surface coverage and dispersion; mechanical robustness; and efficient recovery processability from urban mine.

To fabricate the stable and robust MSAs design, the monofunctionalization of the wagon wheel inner pore surface or successive inclusion of different ligands (*i.e.*, L1, L2, and L3; **Figures 3-5**) into the HOM scaffolds can be achieved by pressure-assisted co-condensation; the high-order hybrids MSA-1 and MSA-3 were obtained using L1 and L3, respectively. Controlled design of MSA-2 was based on the fine-tuned surface patterning of the mesoscopic wagon wheel scaffolding architectures. This was accomplished by using a dispersible active agent (DDAB) that led to the dense decoration of L2 signaling centers inside the wagon wheel pore cavities. With these MSA designs, metal ions can interact with organic moieties by noncovalent bonding (*e.g.,* hydrogen bonding), metal coordination, hydrophobic forces, van der Waals forces, π-π interactions, and electrostatic and/or electromagnetic effects (**Figures 3-5**). In sensing assays, nanoengineered MSAs can be triggered by a target Pd(II), Au(III),or Co(II) ion species and transduce measurable optical signals under synergistic pH, reaction temperature, and contact time (response time) conditions, enabling the binding of the metals into a hydrophobic or hydrophilic ligand pocket to be mimicked. The developed MSAs not only removed Pd(II), Au(III), and Co(II) ions from complex environmental matrices but also provided a means for a simple visual colorimetric estimate of the metal ion concentration; UV-vis reflectance spectroscopy sensitively quantified metal ion concentration over a wide range of concentration (**Figures 3-6**). Thus, MSAs provide a simple and sensitive colorimetric-based solution to detect changes over a wide range of metal ion concentrations as well as a means for the sensitive quantification of the target ions, thereby avoiding the need for sophisticated instruments. Even at ultra-trace concentrations (≤0.19 μg/L), a signal change in the reflectance spectra of the sensors appeared during formation of the complexes (**Figure 1**).

In batch sensing/removal/extraction systems, a major advantage of the wagon-wheel-shaped MSAs is their selectivity toward target ions, thereby preventing hindrance from interfering competing ions. **Figure 6** confirmed the selective removal and efficient monitoring of Pd(II), Au(III), and Co(II) ions by the optical MSAs. The negligible change in the reflectance signals of the MSAs in the presence of competing ions indicated that weak chelates were formed between competing metals and L1, L2, and L3, specifically at pH 2, 7, and 5.2, respectively. The selectivity of the MSAs can be ascribed to the formation of highly stable octahedral [Pd-$(L1)_2$], square-planar [Au-(L2)], and octahedral [Co-$(L3)_2$] complexes.

For judging the cost-effectiveness, recyclability and durability of wagon-wheel-shaped MSAs after repeated regeneration/reuse cycles were investigated. **Figure 8** shows that the MSAs retained a high efficiency for detection/removal/extraction of Pd(II), Au(III), and Co(II) ions over repeated regeneration/reuse cycles, although overall efficiency decreased slightly after the sixth regeneration/reuse cycle. The stability of the cubic *Ia*3*d* mesostructure and the incorporation of L1, L2, and L3 into the ordered wagon-wheel-shaped pores (induced by strong H-bonding and dispersive interactions) play significant roles in maintaining the functionality of the ion-sensing/capture system through several regeneration/reuse cycles (see **Figure 7**).

Recovering Pd(II), Au(III), and Co(II) ions from the urban mine can help limit the environmental damage associated with mining these metals, especially with respect to the impact on land and climate. Using real urban mine samples, results have shown that the MSAs described herein can selectively recover Pd and Au from e-waste, and Co from discarded LIBs (**Table 1** & **Figure 9**), but practical, scalable process still remains challenge for the future applicability of the metal recovery from urban mine.

On the basis of the proposed management protocol, two key components play important roles in the enhanced metal ion accessibility, adsorption capacity, and recovery during the heterogeneous processes. First, the large surface-to-volume ratios and open cylindrical pores of the wagon wheel cubic *Ia*3*d* mesostructures (MSAs) promote orientational ligand assembly (as evidenced by the flexible interaction of Pd(II), Au(III), and Co(II) ions with L1, L2, and L3 and the high affinity of the metal-to-ligand binding events) (**Figures 3-5**). Second, the selective adsorption/detection/extraction processes mainly depend on the structure of the chelating agent, the experimental conditions (particularly pH), the composition of the ion system, the metal ion concentrations, and metal-to-ligand binding events. Although this protocol shows significant progress in the quality, and efficiency of the recovery methods, further efforts are required so that they can be used in other demanding applicability of environmental wastes, in which they enriched with high-doses of actively competitive metals such as Cu(II), Fe(III) and Ni(II) ions.

In conclusion, efficient, cost-effective, wagon-wheel-shaped MSAs have developed for recovering palladium, gold and cobalt metals from the urban mine. Results show evidence that MSAs will be useful in providing a route to a sustainable supply of gold, palladium, and cobalt to meet the needs of modern society.

Disclosures

The authors declare that they have no competing financial interests.

Acknowledgements

This work was supported by the Ministry of Education, Culture, Sports, Science & Technology and the Ministry of Environment, Government of Japan.

References

1. Chung, S-W., & Murakami-Suzuki, R. A Comparative study of e-waste recycling systems in Japan, South Korea and Taiwan from the EPR perspective: Implications for Developing Countries. Michikazu Kojima (ed.), *Promoting 3Rs in developing countries-Lessons from the Japanese experience.* Institute of Developing Economies, JETRO. 125-145, ISBN 978-4-258-58030-9 (2008).
2. Li, J., Lu, H., Guo, J., Xu, Z., & Zhou, Y. Recycle technology for recovering resources and products from waste printed circuit boards, *Environ. Sci. Technol.* **41**(6) 1995-2000 (2007).
3. Ammen, C. W. *Recovery and Refining of Precious Metals.* Springer, New York, 99-138 (1984).

4. Hageluken, C. Recycling the platinum group metals: A European Perspective, *Platinum Metals Rev.* **56** (1), 29-35 (2012).
5. Hall, W. J., & Williams, P. T. Separation and recovery of materials from scrap printed circuit boards. *Resour. Conserv. Recy.* **51** (3), 691-709 (2007).
6. Tuncuk, A., Stazi, V., Akcil, A., Yazici, E. Y., & Deveci, H. Aqueous metal recovery techniques from e_scrap: Hydrometallurgy in recycling, *Miner. Eng.* **25** (1), 28-37 (2012).
7. Huang, K., Guo, J., & Xu, Z. Recycling of waste printed circuit boards: A review of current technologies and treatment status in China, *J. Hazard. Mater.* **164** (2-3), 399-408 (2009).
8. Oh, C.J., Lee, S.O., Yang, H.S., Ha, T.J., & Kim, M.J. Selective leaching of valuable metals from waste printed circuit boards. *J. Air Waste Manage.* **53** (7), 897-902 (2003).
9. Birloaga, I., De Michelis, I., Ferella, F., Buzatu, M., & Vegliò, F. Study on the influence of various factors in the hydrometallurgical processing of waste printed circuit boards for copper and gold recovery. *Waste Manage.* **33** (4), 935-941 (2013).
10. Park, Y. J., & Fray, D. J. Recovery of high purity precious metals from printed circuit boards. *J. Hazard. Mater.* **164** (2-3), 1152-1158 (2009).
11. El-Safty, S. A., Shenashen, M. A., Ismael, M., Khairy, M., & Awual, M. R. Optical mesosensors for monitoring and removal of ultra-trace concentration of Zn(II) and Cu(II) ions from water. *Analyst.* **137** (22), 5208-5214 (2012).
12. El-Safty, S. A., Shenashen, M.A., Ismael, M., Khairy, M., & Awual, M. R. Mesoporous aluminosilica sensors for the visual removal and detection of Pd(II) and Cu(II) ions., *Microporous Mesoporous Mater.* **166**, 195-205 (2013).
13. Khairy, M., El-Safty, S. A., & Shenashen, M. A. Environmental remediation and monitoring of cadmium, *TrAC Trends Anal. Chem.* **62**, 56-68 (2014).
14. Elci, L., Soylak, M., & Buyuksekerci, E. B. Separation of gold, palladium and platinum from metallurgical samples using an amberlite XAD-7 resin column prior to their atomic absorption spectrometric determination. *Anal. Sci.* **19** (12), 1621-1624 (2003).
15. Medved, J., Bujdos, M., Matus, P., & Kubova, J. Determination of trace amounts of gold in acid-attacked environmental samples by atomic absorption spectrometry with electrothermal atomization after preconcentration, *Anal. Bioanal. Chem.* **379** (1), 60-65 (2004).
16. Liu, P., Pu Q., & Su, Z. Synthesis of silica gel immobilized thiourea and its application to the on-line preconcentration and separation of silver, gold and palladium, *Analyst.* **125** (1), 147-150 (2000).
17. El-Safty, S. A. Functionalized hexagonal mesoporous silica monoliths with hydrophobic azo- chromophore for enhanced Co(II) ion monitoring. *Adsorption.* **15** (3), 227-239 (2009).
18. Zhao, J. M., Shen, X. Y., Deng, F. L., Wang, F. C., Wu, Y., & Liu, H. Z. Synergistic extraction and separation of valuable metals from waste cathodic material of lithium ion batteries using Cyanex272 and PC-88A. *Sep. Purf. Technol.* **78** (3), 345-351 (2011).
19. Swain, B., Jeong, J., Lee, J. C., Lee, G. H., & Sohn, J.S. Hydrometallurgical process for recovery of cobalt from waste cathodic active material generated during manufacturing of lithium ion batteries, *J. Power Sources.* **167** (2), 536-544 (2007).
20. El-Safty, S. A., Awual, M. R., Shenashen, M. A., Shahat, A. Simultaneous optical detection and extraction of cobalt(II) from lithium ion batteries using nanocollector monoliths, *Sens. Actut. B Chem.* **176**, 1015-1025, (2013).
21. Barefoot, R. R., & Van Loon, J. C. Recent advances in the determination of the platinum group elements and gold. *Talanta.* **49** (1), 1-14 (1999).
22. Gureva, R. F., & Savvin, S. B. Spectrophotometric methods for determining noble metals, *J. Anal. Chem.* **57** (11), 980-996 (2002).
23. Zhang, S., Pu, Q., Liu, P., Sun, Q., & Su, Z. Synthesis of amidinothioureido-silica gel and its application to flame atomic absorption spectrometric determination of silver, gold and palladium with on-line preconcentration and separation, *Anal. Chim. Acta.* **452** (2), 223-230 (2002).
24. Hinds, M. Determination of gold, palladium and platinum in high purity silver by different solid sampling graphite furnace atomic absorption spectrometry methods, *Spectrochim. Acta B.* **48** (3), 435-445 (1993).
25. Elshehy, E. A., El-Safty, S. A., Shenashen, M. A., & Khairy, M. Design and evaluation of optical mesocaptor for the detection/recovery of Au(III) from an urban mine, *Sens. Actuat. B Chem.* **203**, 363-374 (2014).
26. Safavi A., & Shams, E. Highly sensitive and selective measurements of cobalt by catalytic adsorptive cathodic stripping voltammetry. *Talanta.* **51** (6), 1117-1123 (2000).
27. Singh, A. K., Mehtab, S., Saxena, P. A novel potentiometric membrane sensor for determination of Co^{2+}based on 5-amino-3-methylisothiazole *Sens. Actut. B-Chem.* **120** (2), 455-461 (2007).
28. Shenashen, M. A., Elshehy, E. A., El-Safty, S. A., & Khairy, M. Visual monitoring and removal of divalent copper, cadmium, and mercury ions from water by using mesoporous cubic Ia3d aluminosilica sensors. *Sep. Purif. Technol.* **116**, 73-86 (2013).
29. Shenashen, M. A., El-Safty, S. A., & Elshehy, E. A. Architecture of optical sensor for recognition of multiple toxic metal ions from water. .*J. Hazard. Mater.* **260**, 833-843 (2013).
30. Khairy, M., El-Safty, S. A., Shenashen M. A., & Elshehy, E. A. Hierarchical inorganic-organic multi-shell nanospheres for intervention and treatment of lead-contaminated blood. *Nanoscale.* **5** (17), 7920-7927 (2013).
31. El-Safty, S. A., Khairy, M., & Ismael, M. Visual detection and revisable supermicrostructure sensor systems of Cu(II) analytes. *Sens. Actut. B-Chem.* **166-167**, 253-263 (2012).
32. Rampazzo, E., Brasola, E., Marcuz, S., Mancin, F., Tecilla, P., & Tonellato, U. Surface modification of silica nanoparticles: a new strategy for the realization of self-organized fluorescence chemosensors, *J. Mater. Chem.* **15** (27-28), 2687-2696 (2005).
33. Han, W. S., Lee, H. Y., Jung, S.H., Lee, S. J., & Jung, J. H. Silica-based chromogenic and fluorogenic hybrid chemosensor materials. *Chem. Soc. Rev.* **38** (7), 1904-1915 (2009).
34. Shenashen, M. A., El-Safty, S. A., Elshehy, E. A., & Khairy, M. Hexagonal-prism-shaped optical sensor/captor for the optical recognition and sequestration of Pd^{II} ions from urban mines, *Eur. J. Inorg. Chem.* **2015**, 179-191 (2015).
35. Ros-Lis, J. V., Casasus, R., Comes, M., Coll, C., Marcos, M. D., Martinez-Manez, R., Sancenon, F., Soto, J., Amoros, P., El Haskouri, J., Garro, N., & Rurack, K. A mesoporous 3D hybrid material with dual functionality for Hg^{2+} detection and adsorption. *Chem. Eur. J.* **14**, 8267-8278 (2008).
36. Jung, J. H., Lee, J. H., & Shinkai, S. Functionalized magnetic nanoparticles as chemosensors and adsorbents for toxic metal ions in environmental and biological fields. *Chem. Soc. Rev.* **40** (9), 4464-4474 (2011).
37. El-Safty, S. A., & Hanaoka, T. Microemulsion liquid crystal templates for highly ordered three-dimensional mesoporous silica monoliths with controllable mesopore structures. *Chem. Mater.* **16** (9), 384-400 (2004).
38. El-Safty, S. A., & Hanaoka, T. Fabrication of crystalline, highly ordered three-dimensional silica monoliths (HOM-n) with large, morphological mesopore structures. *Adv. Mater.* **15** (22), 1893-1899 (2003).

39. El-Safty, S. A., & Hanaoka, T. Monolithic nanostructured silicate family templated by lyotropic liquid-crystalline nonionic surfactant mesophases. *Chem. Mater.* **15** (22), 2892-2902 (2003).
40. Balaji, T., El-Safty, S. A., Hanaoka, T., Matsunaga, H., Mizukami, F. Optical sensors-based nanostructured cage materials for detection of toxic metal ions. *Angew. Chem. Int. Ed.* **45** (43), 7202-7208 (2006).
41. Huang, J., Gao, X., Jia, J., Kim, J-K., & Li, Z. Graphene oxide-based amplified fluorescent biosensor for Hg^{2+} detection through hybridization chain reactions, *Anal. Chem.* **86** (6), 3209-3215 (2014).
42. El-Safty, S. A., Shenashen, M. A., Ismael M., & Khairy, M. Mesocylindrical aluminosilica monolith biocaptors for size-selective macromolecule cargos. *Adv. Funct. Mater.* **22** (14), 3013-3021 (2012).
43. Kreno, L. E., Leong, K., Farha, O. K., Allendorf, M., Van Duyne, R. P., & Hupp, J. T. Metal Organic Framework Materials as Chemical Sensors, *Chem. Rev.* **112** (3), 1105-1125 (2012).
44. El-Safty, S. A., Hanaoka, T., & Mizukami, F. Large scale design of cubic la3d mesoporous silica monoliths with high order, controlled pores, and hydrothermal stability. *Adv. Mater.* **17** (1), 47-53 (2005).
45. El-Safty S. A., & Shenashen, M. A. Mercury-ion optical sensors. *Trends Anal. Chem.* **38** (1), 98-115 (2012).
46. El-Safty, S. A., Shenashen, M. A., & Ismail, A. A. A multi-pH-dependent, single optical mesosensor/captor design for toxic metals. *Chem. Commun.* **48** (77), 9652-9654 (2012).
47. Shenashen, M. A., El-Safty, S. A., & Elshehy, E. A. Monolithic scaffolds for highly selective ion sensing/removal of Co(II), Cu(II), and Cd(II) ions in water. *Analyst.* **139**(24), 6393-6405 (2014).